A Gaussian beam shooting algorithm for radar propagation simulations

Ihssan Ghannoum, Christine Letrou, Gilles Beauquet

A GAUSSIAN BEAM SHOOTING ALGORITHM FOR RADAR PROPAGATION SIMULATIONS

Ihssan Ghannoum and Christine Letrou
Lab. SAMOVAR (UMR CNRS 5157)
Institut TELECOM SudParis
9 rue Charles Fourier, 91011 Evry Cedex, France
Emails: ihssan.ghannoum@it-sudparis.eu
christine.letrou@it-sudparis.eu

Gilles Beauquet
Surface Radar
THALES Air Systems S.A.
Hameau de Roussigny, 91470 Limours, France
Email: gilles.beauquet@thalesgroup.com

***Abstract*— Gaussian beam shooting is proposed as an alternative to the Parabolic Equation method or to ray-based techniques, in order to compute backscattered fields in the context of Non-Line-of-Sight ground-based radar. Propagated fields are represented as a superposition of Gaussian beams, which are launched from the emitting antenna and transformed through successive interactions with obstacles. In this paper, we present an outline of this 3D algorithm and propose a beam re-expansion scheme to address the problem of beam widening. Realistic scenarios will be used to test the ability of Gaussian beam shooting to accommodate typical propagation environments for ground-based UHF radar, including buildings.**

Keywords - Radar; 3D propagation; Gaussian beam shooting

I. INTRODUCTION

When ground-based radars operate in built-up environments, propagation scenarios are likely to involve Non-Line-of-Sight (NLOS) targets and backscattering through multiple reflexions [1]. Computation of fields backscattered from NLOS target is hardly possible with Parabolic Equation. Ray based techniques are well suited in multipath environments but they rely on far field assumptions which are not always valid, they suffer from caustics problems in the presence of concave surfaces or refractivity, and they become computationally intensive in 3D environments. Iterative Physical Optics offers a caustic free alternative, but at the expense of even higher computational burden.

Due to their paraxial nature, Gaussian beam (GB) propagators offer an alternative to overcome these limitations. Their use is however subject to specific constraints and raises problems which will be addressed in this paper.

”Gaussian beams are paraxial” means that their fields are localized around a beam axis, both in spatial coordinates and in the transform (spectral) domain of wave-vector directions: Gaussian beams can be viewed as ”big rays”, as shown in Fig. 1. Their ”width”, defined as the radius of the region around the beam axis where beam fields are considered non negligible, has a finite value both in space and in transform domain.

Thereof GBS algorithms possess the following interesting features:

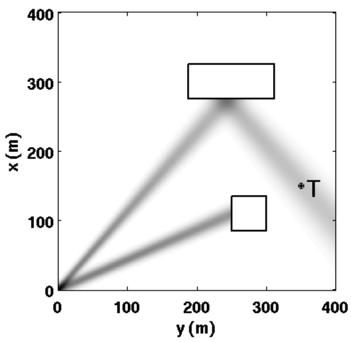

Fig. 1. Gaussian beam propagation in a NLOS configuration: 2D cut for two beams propagating in the xOy plane (taken at some height above the ground), launched from a source centered at the origin in the xOz plane. A beam is reflected by a rectangular ”building” and incident on the target ”T”, the other is obstructed by a square obstacle. Darkness is proportional to field amplitude.

- Emitted fields can be represented with less beams than rays, and this discretization, based on frame decomposition (cf Section II), does not introduce any non physical discontinuities.
- GB tracking through multiple bounces is performed by following the beam axis paths only, and by computing the transformation operators (reflexion, refraction) along the beam axes [2].
- No far field approximation is required to establish paraxial GB formulas, which rely only on paraxial approximations.
- GB width cannot be reduced to zero, which prevents the appearance of caustics.
- The finite size of obstacles is to some extent automatically accounted for, as beams are themselves of finite transverse dimensions. A beam whose field in negligible on an obstacle interface is not affected by the presence of this obstacle (contrary to geometrical optics rays, which must be supplemented by diffracted rays). ”Diffraction” effects are thus partly modelled without any additional complexity [3].

All these features make GBS particularly well suited for propagation simulations in dense multipath 3D environments. Its efficiency has already been tested for 3D indoor channel simulations in the millimeter wave domain [4]. In the following, figures will however present 2D cuts of 3D GBS scenarios for the sake of clarity.

These advantageous features are however balanced by an unavoidable counterpart: for a GB to be paraxial, its "width" must be large enough in the plane of its minimum, typically several wavelengths. Even more, the larger the "beam width", the more collimated the beam. In Fig. 2 and in all following figures, colored surfaces correspond to regions where beam fields are considered as non negligible. Visibly, smaller initial beam width leads to more diverging beam. Collimation is highly desirable, as it guarantees the localization of beam fields around the beam axis within reasonable distance, even after propagation along large distances. It also insures the accuracy of paraxial beam formulas.

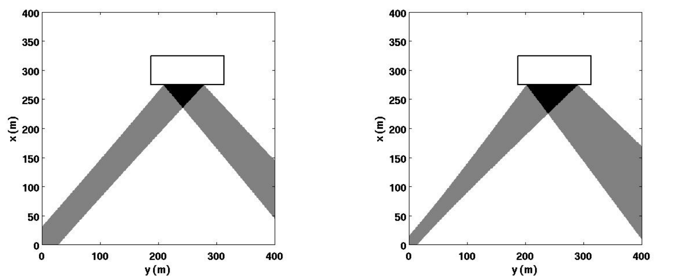

Fig. 2. Gaussian beam propagation and reflexion: 2D cut for a beam launched in xOy plane from a source centered at the origin in the xOz plane with a minimum width of 21λ, e.g. 14.7 m at 430 MHz (left) and 10.5λ, e.g. 7.35 m at 430 MHz (right). Colored surfaces correspond to regions where beam fields are considered as non negligible.

Due to this constraint, all propagation scenarios are not amenable to GBS algorithms. For instance, propagation at wavelengths larger than one meter in an office building with small office rooms can hardly be simulated with Gaussian beams.

In order to extend the range of applicability and the accuracy of GBS algorithms, we propose to perform re-expansions of beam fields into new sets of GB when the beam width becomes too large as compared to the typical dimensions of the environment, or when a beam comes across a discontinuity (e.g. building corner). The proposed re-expansion algorithm has already been validated in two dimensions, in the case of beam partial obstruction by an absorbing plane [5].

Section II outlines the basics of frame based decomposition of radiated fields into paraxial GB, and GB tracking. Section III then proposes a re-expansion algorithm to accommodate GB widening and diffraction. In the full paper, an additional Section will present results obtained with the GBS algorithm in a realistic radar scenario.

II. Gaussian beam launching and tracking

Let us assume that the near field of a radar antenna has been measured in a plane situated in front of the antenna. This planar distribution will be used as the equivalent source field. Frame-based beam launching is then performed through two successive steps:

- The planar distribution of source fields is expressed as a weighted sum of Gaussian windows which form a "frame" (cf Subsection II-A).
- Each Gaussian window radiates in the form of a Gaussian beam (cf Subsection II-B).

A. Source frame decomposition

The frame windows $\psi_\mu(x,z)$ used to describe a planar source distribution in the xOz plane are constructed as the product of frame windows $\psi^x_{m,n}(x)$ and $\psi^z_{p,q}(z)$ in $L_2(\mathbb{R})$:

$$\psi_\mu(x,z) = \psi^x_{m,n}(x)\psi^z_{p,q}(z) \tag{1}$$

where $\mu = (m,n,p,q)$ is a composite translation index in $\mathbb{Z}^4$. The frame windows $\psi^x_{m,n}(x)$ are obtained by translation of a Gaussian function $\psi(x)$ along the spatial coordinate x and along its spectral counterpart k_x:

$$\psi^x_{m,n}(x) = \psi(x - m\bar{x})e^{in\bar{k}_x x} \tag{2}$$

- $\bar{x}$ and $\bar{k}_x$ are respectively the spatial and spectral translation steps, m and n the spatial and spectral translation indices.
- $\{\psi_\mu,\ \mu \in \mathbb{Z}^2\}$ is a frame if and only if $\bar{x}\bar{k}_x = 2\pi\nu$, with $\nu < 1$ (ν: oversampling factor).
- the favorite choice for the translation steps is: $\bar{x} = \sqrt{\nu}L$, $\bar{k}_x = \sqrt{\nu}(2\pi/L)$ ("balanced" frame).

The same construction is used for the frame along z, with p, q the spatial and translation indices along z. In the following, the Gaussian function ψ is taken as:

$$\psi(x) = \left(\sqrt{2}/L\right)^{\frac{1}{2}}\ e^{-\pi\left(\frac{x}{L}\right)^2} \tag{3}$$

It is centered at $x = 0$, and L defines the window width. In the following, the window field will be considered as negligible for $x > L\sqrt{2/\pi}$.

According to frame theory, a linearly polarized component ($U = E_x$ or $U = E_z$) of the E-field distribution in the source plane $y = 0$ can be expressed as a weighted summation of the $\psi_{\boldsymbol{\mu}}$ frame windows:

$$U(x,z) = \sum_{\boldsymbol{\mu}} A_{\boldsymbol{\mu}}\psi_{\boldsymbol{\mu}}(x,z)\ ,\ \boldsymbol{\mu} = (m,n,p,q) \in \mathbb{Z}^4 \tag{4}$$

The $A_{\boldsymbol{\mu}}$ coefficients are obtained by projection of the distribution on the "dual frame" windows $\varphi_{\boldsymbol{\mu}}(x,z)$=$\varphi^x_{m,n}(x)\varphi^z_{p,q}(z)$. For a balanced frame with $\nu \leq 0.25$, $\varphi(u) \sim \frac{\nu}{\|\psi\|^2}\psi(u)$ with

$u = x, z$, hence:

$$A_{\boldsymbol{\mu}} = \int_{-\infty}^{\infty} U(x,y)\ \varphi_{\boldsymbol{\mu}}^{\times}(x,z)\ dxdz \qquad (5)$$
$$= \int_{-\infty}^{\infty}\int_{-\infty}^{\infty} U(x,z)\ \frac{\nu_x}{\|\psi\|^2}[\psi_{m,n}^{x}(x)]^{\times} \cdot \frac{\nu_z}{\|\psi\|^2}[\psi_{p,q}^{z}(z)]^{\times}\ dxdz$$

It must be noted that if a set of Gaussian windows is a frame, the set of their Fourier transforms is also a frame. The windows of this transformed frame are also Gaussian, and translated along spectral and spatial variables. As a consequence, the field radiated by a given antenna can also be decomposed on a frame in the spectral domain, if the antenna plane wave spectrum is known. In most cases, the antenna plane wave spectrum is easily derived from the far field radiation pattern. This spectral domain decomposition leads to the same decomposition coefficients as the spatial domain decomposition. The choice of either domain for frame decomposition is a matter of convenience, related to available antenna data (near field or far field).

B. Frame window radiation

Through paraxial asymptotic evaluation of plane wave spectrum integrals, the fields radiated by the source field distributions $\psi_{\boldsymbol{\mu}}(x,z)$ (either for x or z component) are put in the form of paraxial Gaussian beams. Let us denote $\boldsymbol{B}_{\boldsymbol{\mu}}(\boldsymbol{r})$ the field radiated at point $\boldsymbol{r}$. The paraxial expression of $\boldsymbol{B}_{\boldsymbol{\mu}}$ is:

$$\boldsymbol{B}_{\boldsymbol{\mu}}(\boldsymbol{r})=\boldsymbol{B}_0\sqrt{\frac{\det \boldsymbol{\Gamma}^{-1}(0)}{\det \boldsymbol{\Gamma}^{-1}(y_{\boldsymbol{\mu}})}}\exp ik\Big[y_{\boldsymbol{\mu}} + \tfrac{1}{2}\boldsymbol{x}_{\boldsymbol{\mu}}^{t}\boldsymbol{\Gamma}(y_{\boldsymbol{\mu}})\boldsymbol{x}_{\boldsymbol{\mu}}\Big] \quad (6)$$

with $\boldsymbol{B}_0$ a vector depending on the source polarization. This expression is analog to that of a geometrical optics ray along the $y_{\boldsymbol{\mu}}$ direction, with $\boldsymbol{\Gamma}$ the curvature matrix and $\sqrt{\frac{\det \boldsymbol{\Gamma}^{-1}(0)}{\det \boldsymbol{\Gamma}^{-1}(y_{\boldsymbol{\mu}})}}$ the divergence factor. $\boldsymbol{x}_{\boldsymbol{\mu}} = (x_{\boldsymbol{\mu}}, z_{\boldsymbol{\mu}})$ is the position vector of the point $\boldsymbol{r}$ in a plane transverse to the $y_{\boldsymbol{\mu}}$ axis.

The difference between geometrical optics rays and Gaussian beams stems from the fact that $\boldsymbol{\Gamma}$ is a real matrix in the first case, a complex one in the latter. This complex matrix accounts for the Gaussian decay of fields with increasing distance from the $y_{\boldsymbol{\mu}}$ axis in transverse planes. The $y_{\boldsymbol{\mu}}$ axis is then called the beam axis.

The frame decomposition of source fields given in (4) leads then to the expression of radiated fields $\boldsymbol{E}(\boldsymbol{r})$ (for $y > 0$) as a summation of propagating Gaussian beams:

$$\boldsymbol{E}(\boldsymbol{r}) = \sum_{\boldsymbol{\mu}} A_{\boldsymbol{\mu}}\boldsymbol{B}_{\boldsymbol{\mu}}(\boldsymbol{r}) \qquad (7)$$

Fig. 3 presents a subset of source beam fields launched from a number of frame windows. The beam axis origins (resp. directions) are determined by the m, p spatial (resp. n, q spectral) translation indices of source windows.

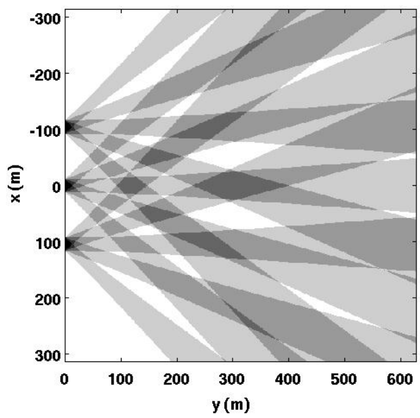

Fig. 3. Frame based Gaussian beam launching: non negligible field regions (2D cut in the xOy plane) for beams radiated by frame windows in the xOz plane, with $L_x = 15\lambda$ at 430MHz (8.35m initial beam width) and translation indices $m = -10, 0, 10$ and $n = -20, -10, 0, 10, 20$ ($p = q = 0$).

C. Gaussian beam tracking

The GBS algorithm really starts with the tracking of beam axes within the environment. Only beams which are significantly excited (frame coefficients with values higher than a given threeshold) need to be tracked. Reflected or refracted beams are expressed as beams originating in "image" source distributions [6].

In the case of beams impinging on discontinuities such as in Fig. 4, we propose to perform the beam re-expansion described in the next Section, and which guarantees the paraxiality of emerging beams. The same re-expansion algorithm will also be of great use to re-expand beams after a long propagation distance, when paraxial formulas are no longer accurate.

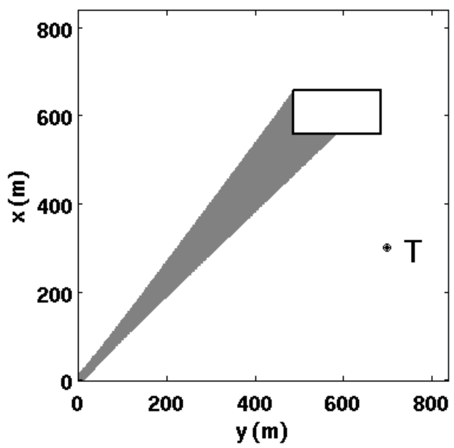

Fig. 4. Gaussian beam impinging on a discontinuity: 2D cut for a beam propagating in the xOy plane, launched from a frame window source centered at the origin in the xOz plane (7.36m beam width at 430MHz) and incident on a rectangular "building". "T" denotes the target.

III. Beam re-expansion algorithm

In this section we address the problem of beam re-expansion in the course of a GBS algorithm. We propose a two-step solution:

1) Decompose the field of interest on a frame of (spatially) narrow windows in the plane of re-decomposition.
2) Through a matrix vector multiplication, perform a change of frame and obtain the frame coefficients of the field of interest on a frame of (spatially) wide windows, which will be used to track fields further in the form of collimated beams.

If we denote by:

- $\underline{A}'_{\mu'}$ the vector of narrow window frame coefficients of the field of interest,
- $C_{\mu}^{\mu'}$ the matrix of frame change, with μ' the narrow window indices and μ the window indices in the final frame (wide windows),
- $\underline{A}_{\mu}$ the vector of wide window frame coefficients of transformed and diffracted field,

the re-expansion algorithm can be summarized by:

$$\underline{A}_{\mu} = C_{\mu}^{\mu'} \underline{A}'_{\mu'}$$

A schematic representation of this re-expansion algorithm is given in Fig. 5. The frame of spatially narrow windows is schematically represented on the left of the re-decomposition plane, the frame of spatially wide (spectrally narrow) windows is schematically represented on the right of the re-decomposition plane. The latter windows radiate in the form of "new" collimated beams, launched from the re-decomposition plane.

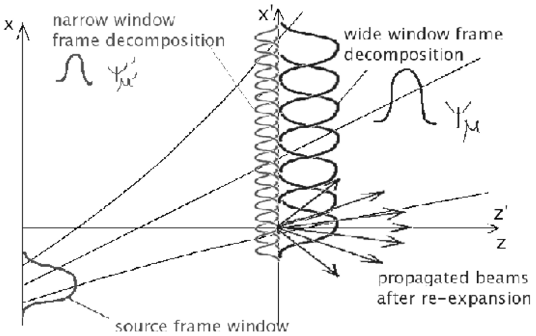

Fig. 5. Field re-expansion scheme in a plane.

The use of an intermediate frame of narrow windows is of particular interest for two reasons. First, if the ratio between the width of wide windows (including source frame windows) and narrow windows is large enough, the $A'_{\mu'}$ decomposition coefficients and the elements of the $C_{\mu}^{\mu'}$ frame change matrix can be expressed in closed form, owing to paraxial approximations in projection integral evaluations [5]. Secondly, the truncation of fields along a discontinuity is straighforward, simply equating to zero the $A'_{\mu'}$ narrow window frame coefficients in the region where fields are not the ones "of interest" (either reflected or transmitted). For very narrow windows, this representation of fields on a limited surface is close to the Physical Optics one.

Fig. 6 and Fig. 7 illustrate the new beam launching which results from field re-expansion in the two planes (dashed lines) where incident beam fields are not negligible in the scenario represented in Fig. 4. Not all beams are represented for clarity, but it should also be mentioned that if the region of interest for target position is known, not all "new" beams have to be tracked. Considering the target "T" position, none of the "new beams" emerging from re-expansion in the $P2$ plane on Fig. 6 have to be tracked. Only few of those emerging from re-expansion in the $P1$ plane in Fig. 7 have to be tracked.

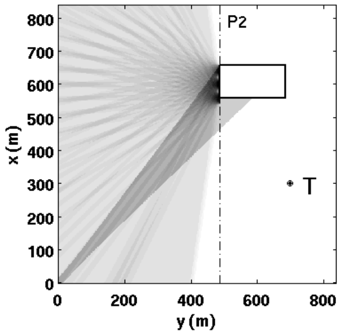

Fig. 6. Incident beam and new beam launching after re-expansion in plane $P2$. Same configuration as in Fig. 4.

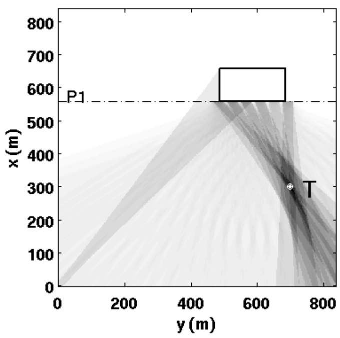

Fig. 7. Incident beam and new beam launching after re-expansion of reflected fields in plane $P1$. Same configuration as in Fig. 4. Beams incident on the target are dark grey.

IV. Numerical results

In this section, first numerical results illustrate the use of the re-decomposition algorithm to represent fields intercepted by limited planar surface obstacles, such as building walls.

Fig. 8 shows the incident field level of a collimated beam launched from a source frame and intercepted by a lateral obstacle (rectangular surface).

The source frame is defined in the xOz plane of the global coordinate system, with $L_x = L_z = 10\lambda$ (7 m at 430 MHz; collimation distance $b_0 \sim 70$ m) defining the width of the frame windows and $\nu = 0.16$ the oversampling factor. The

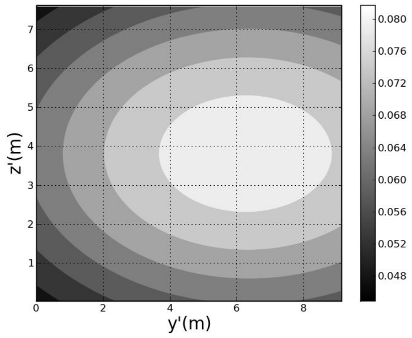

Fig. 8. Magnitude of the reference incident beam field on a lateral rectangular surface.

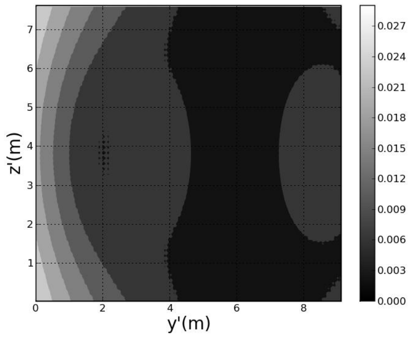

Fig. 10. Normalized absolute error for the incident field obtained by frame summation with narrow windows after incident field re-decomposition. Same rectangular surface and incident beam as in Figs. 8 and 9.

incident beam is radiated by the $\psi_{\boldsymbol{\mu}}(x,z)$, $\boldsymbol{\mu} = (m,n,p,q)$, frame window with $m = p = q = 0$ and $n = 15$, which means that the beam axis makes a $48\,\text{deg}$ angle with the y axis in the horizontal xOy plane.

The rectangular surface where the incident beam field is computed is in the vertical lateral zOy plane defined by $x = 76.3$ m. The width of this "wall" is approximately 9.1 m (horizontal dimension along y) and its height 7.6 m (vertical dimension along z). The distance between the origin of the incident beam axis and its incidence point on the wall is about 115 m. The narrow window frame on the rectangular plate is defined by $L_{y'} = L_{z'} = 0.5\lambda$ and $\nu = 0.16$.

Figs. 9 and 10 present the absolute error of the incident field computed with paraxial beam formulas and with frame summation of the narrow frame windows after incident field re-decomposition, respectively. The error is normalized to the maximum of the field magnitude on the rectangle.

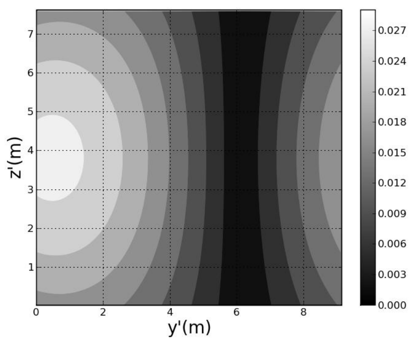

Fig. 9. Normalized absolute error for the incident field obtained with paraxial beam formulas. Same rectangular surface and incident beam as in Fig. 8.

From these figures it appears that the re-decomposition algorithm provides accurate enough results. The accuracy of the results is better than the one obtained with paraxial beam propagation formulas at distances along the beam axis where they are usually considered as reasonably accurate (less than twice the collimation distance).

It has been observed (not shown here) that the frame change from spatially narrow to spatially wide windows does not degrade this accuracy. Other results showing the obtained accuracy for the fields reflected by the wall will be presented at the conference.

V. CONCLUSION

In this paper, a 3D Gaussian beam shooting algorithm has been proposed to overcome the limitations encountered by other methods in the context of ground-based NLOS radar. This algorithm is based on a frame decomposition of emitted fields followed by a Gaussian beam tracking procedure. The Gaussian beam paraxiality leads to "automatic" grouping of rays, which are collectively propagated and transformed along beam axis paths, leading to efficient and straightforward algorithms. The problem of beam widening is addressed with a new re-expansion formulation. Playing with successive interchanges between wide and narrow frame windows provides a simple, yet approximate, Physical Optics like treatment of diffraction and more generally of localized field transformations (for instance by non planar surfaces). This algorithm will be applied to 3D simulations of radar field propagation in a realistic scenario of UHF ground-based radar application.

REFERENCES

[1] O. Adrian, J.-M. Ferrier, Y. Ricci, "Combination of NLOS Radar Technology and LOS Optical Technology for Defence and Security", *The Institution of Engineering and Technology International Conference on Radar Systems (RADAR 2007),* Edinburgh, UK, Oct. 2007.

[2] E. Heyman, and L. Felsen, "Gaussian beam and pulsed beam dynamics: complex source and spectrum formulations within and beyond paraxial asymptotics", *J. Opt. Soc. Amer. A*, *18*, 1588–1610, 2001.

[3] D. Lugara, C. Letrou, A. Shlivinski, E. Heyman, A. Boag, "Frame-based Gaussian beam summation method: theory and applications," *Radio Science,* vol. 38, no. 2, 8026, 2003.

[4] A. Fluerasu, "Modélisation de champs dans le domaine spatio-temporel par une méthode de frame de Gabor. Application à la caractérisation du canal indoor millimétrique," *PhD,* Université de Marne-la-Vallée, 2003.

[5] C. Letrou, "A Gaussian beam shooting scheme for fast multidimensional physical simulation of propagation channels in wireless communication systems," *International Conference on Electromagnetics in Advanced Applications (ICEAA '07),* Torino, Italy, 2007.

[6] R. Tahri, C. Letrou, V. Fouad Hanna, "A beam launching method for propagation modeling in multipath contexts," *Microwave and Optical Technology Letters,* vol. 35, no. 1, pp. 6–10, 2002.